oral

MDPI

Article

Three-Dimensional Finite Element Analysis on Mandibular Biomechanics Simulation under Normal and Traumatic Conditions

Mihaela Hedeșiu [1], Dan George Pavel [2], Oana Almășan [3,*], Sorin Gheorghe Pavel [4], Horia Hedeșiu [5] and Dan Rafiroiu [6]

[1] Department of Oral and Maxillofacial Surgery and Implantology, Iuliu Hațieganu University of Medicine and Pharmacy, 32 Clinicilor Street, 400029 Cluj-Napoca, Romania
[2] Faculty of Medicine and Pharmacy, University of Oradea, 10 Piaţa 1 Decembrie Street, 410087 Oradea, Romania
[3] Department of Prosthetic Dentistry and Dental Materials, Iuliu Hațieganu University of Medicine and Pharmacy, 32 Clinicilor Street, 400006 Cluj-Napoca, Romania
[4] Department of Electroenergetics and Management, Faculty of Electrical Engineering, Technical University of Cluj-Napoca, 26-28 George Bariţiu Street, 400027 Cluj-Napoca, Romania
[5] Department of Electrical Machines, Marketing & Management, Technical University of Cluj-Napoca, 26-28 George Bariţiu Street, 400027 Cluj-Napoca, Romania
[6] Department of Electrotechnics and Measurements, Faculty of Electrical Engineering, Technical University of Cluj-Napoca, 26-28 George Bariţiu Street, 400027 Cluj-Napoca, Romania
* Correspondence: oana.almasan@umfcluj.ro

Abstract: The main objective was to examine the biomechanical behavior of the mandible under standardized trauma and to develop models of biomechanical responses when the mandible is subjected to various simulated impacts. A homogenous model based on the bone's average mechanical properties was used. To simulate external loads on the mandible, forces on the chin, forces in an anteroposterior direction, and forces from the basilar edge were applied. To simulate mandibular biomechanics, we employed a model created in the ANSYS v19.0 software. The skull with the temporomandibular joint (TMJ) from the Grabcad website was used as the geometric mandibular model. We attempted to simulate the stresses developed in the mandible by impact forces. The amount of force (F) corresponded to the fall of a five-kilogram body (the head), from a height of two meters (F = 6666.7 N). The impact force was applied perpendicular to an arbitrary surface of an area of 10^{-3} m^2. Impact on the chin region and lateral impact on the mandible, from the basilar edge to the gonion were examined. The investigated clinical situations were mandibular complete dentition; jaw with missing mandibular molars; missing third molar and first and second premolars; missing canine, third molar, first and second premolars, and complete edentation. In a normal bite, the highest stress was on the TMJ area. In case of impact on the chin, in complete edentation, a mandibular fracture occurred; in case of impact on the gonion, all stress values exceed the limit value above which the mandible in the condyle area may fracture.

Keywords: mandibular fractures; trauma; jaw injuries; mandibular condyle; finite element

check for updates

Citation: Hedeșiu, M.; Pavel, D.G.; Almășan, O.; Pavel, S.G.; Hedeșiu, H.; Rafiroiu, D. Three-Dimensional Finite Element Analysis on Mandibular Biomechanics Simulation under Normal and Traumatic Conditions. *Oral* **2022**, *2*, 221–237. https://doi.org/103390/oral2030021

Academic Editor: Michele Cassetta

Received: 24 June 2022
Accepted: 17 August 2022
Published: 19 August 2022

Publisher's Note: MDPI stays neutral with regard to jurisdictional claims in published maps and institutional affiliations.

Copyright: © 2022 by the authors. Licensee MDPI, Basel, Switzerland. This article is an open access article distributed under the terms and conditions of the Creative Commons Attribution (CC BY) license (https://creativecommons.org/licenses/by/4.0/).

1. Introduction

1.1. Background

The mandibular fractures are the most common facial fractures with a high prevalence of condylar and subcondylar fractures of the mandible [1–4]. In elderly subjects, mandible fractures occur frequently, with an incidence between 27.8% and 43.3% [5,6]. The fracture site can be the mandible midline, paramedian, body, angle, or condyle [7]. Among the primary causes were reported: assaults and falls, but also occupational factors or sports [8,9]. Males were more affected than females (60% vs. 39.4%) [8,10].

Several studies related to finite element (FE) analysis in condylar base fractures have been published to date but there is still a lack of information regarding the potential changes

induced by the lack of dental units on the biomechanics of mandibular fractures [11–13]. Previous reports showed that FE analysis is a reliable method for the assessment of the biomechanical stability of plate/screw systems used for the mandibular fracture treatment and measurements of stress within mandibular bone induced by various implanting devices' locations and osteosynthesis materials [11,12]. In an experimental study, a simulation of a mandibular trauma was used to examine the fractures caused by an impact to the jaw with and without internal fixation and it was noted that mini-plates may alter the biomechanical behavior of the mandible [13].

Due to the sheer models created by biomechanics, the mathematical computation can be used to analyze complex processes. In the research of bone-breaking strength, an essential property is its mechanical characteristic that represents the relationship between bone deformation and stress, and it is determined by the bone structure [14–19]. The employment of modern computational methods such as FE analysis provides an alternative solution to the physical model that can evaluate complex structures with variable geometry and mechanical properties based on a virtual model [20].

The distribution of stresses and deformations in different sections of the investigated structure should be calculated based on parameters such as internal anatomy and morphological characteristics of the bone [21]. Two different zones of the jaw should be defined on a biomechanical simulation of mandibular fractures: the elastic deformation zone and the plastic zone. The bone fracture movements are also influenced by the occlusal contacts, muscle insertions, and characteristics of the impact [22–24].

Given the fact that mandible fractures occur due to stress in different areas, their treatment involves performing intermaxillary fixation by using different approaches such as semi-rigid internal fixation or osteosynthesis [25]. The current gold-standard treatment for complex mandibular fractures is the placement of osteosynthesis plates, mandibular reconstruction plates can be patient-specific and have a computer-assisted design and manufacturing technology [26]. Titanium plates are used for treating subcondylar fractures [27]. It has been shown that even though the FE method has not been widely applied, the outcomes of in vitro studies on the stable application of two titanium mini-plates in mandibular condyle fractures, were comparable to those of computational studies [28].

To calculate the strength and fatigue of bonding elements used in fracture and defect surgery, a FE model of a mandible with the temporomandibular joint was created and described [29]. FE analysis to compare three different mandible angle fracture treatment methods has been proposed [30]. The more common mandible fracture areas by using a three-dimensional FE method to locate the highest stress lines have been shown and compared with data from clinical experiments [31].

1.2. Objectives

To the best of our knowledge, no study focused on the relation between the biomechanical behavior of the mandible under traumatic situations and the occlusal stops. Since the lateral teeth (molars, premolars) play a significant role in the posterior determinants of occlusion by influencing the curve of Spee, the curve of Wilson, and the occlusal plane, we have chosen to simulate the total deformation and equivalent stress on the surface of the condyle in case of impact with complete dentition, complete edentation, and missing lateral teeth. Due to its function in lateral guidance, we have also considered the situation with the missing canine. Therefore, the objectives of this study were to examine the biomechanical behavior of the jaw under standardized trauma conditions by using FE analysis and computer aided design (CAD) models and to assess the biomechanical response of the normal and partial and total edentulous mandible to stress.

2. Materials and Methods

2.1. Virtual Models for Mandibular Bone

The mandible of the "three-parts Anatomical Skull" model from the GrabCAD website was used in this study as the geometric model [32,33]. This is an articulated lower jaw with

specially designed joints that allow its rotation around fixed axes, rather than an accurate representation of the condyle and the upper joint cavity. The global dimensions of the entire skull were 270 × 200 × 220 mm. Several characteristic distances of the mandible are illustrated in Figure 1. The internal structure of the mandible (alveolus and dental roots, cortical and trabecular bone, respectively) was not represented in our model which was considered homogeneous.

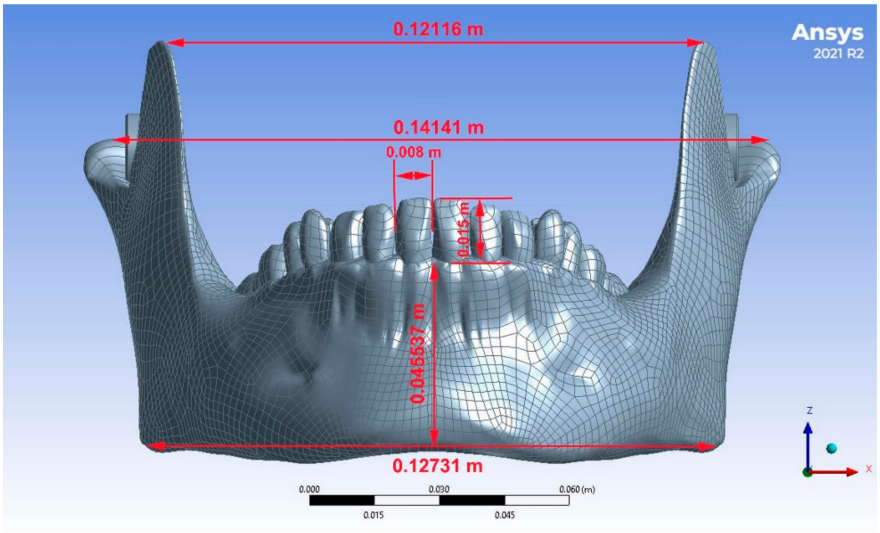

Figure 1. Characteristic dimensions of the mandible with teeth (m = meter).

Average mechanical properties of the cortical and trabecular bone were used for the whole mandible in our model. The mandibular bone, which is primarily made up of trabecular tissue, has a porous structure with a matrix of bone mass and gaps. The total volume of the bone body (TV) comprises the volume of the bone matrix (MV) and the volume of the cancellous bone spaces (VS). The mandible model had a total volume of TV = 0.00017443 m^3 and a total surface area (SA) of 0.04018 m^3.

The volume fraction (VF = MV/TV) and porosity (pV = VS/TV) are used to describe bone structure. The porosities of the cortical and trabecular bone differ. The following values are mentioned in the literature: 50–90% for trabecular bone and 5–10% for cortical bone [34].

Thus, the bone density is an apparent one and could be calculated based on the density of tissues in the bone matrix and the spaces, qm, and qs, respectively: q = (qm × MV + qs × VS)/TV. Although the two partial densities are known from the literature, the two partial volumes MV and VS are not known in our case. Still, knowing that the average thickness of the cortical tissue is Hcort = 1.35 mm and multiplying this value with the surface area of the mandible SA, one can get an estimate of the cortical bone volume: Vcort = Hcort × SA = 55 × 10^{-6} m^3. Subtracting this from the total volume equals the volume of the trabecular tissue: Vtrab = TV–Vcort = 125 × 10^{-6} m^3. Knowing from the literature that the densities of the cortical and trabecular tissues are qcort = 1740 Kg/m^3 and qtrab = 700 Kg/m^3, the average density of the homogeneous mandible could be approximated as qave = (qcort × Vcort + qtrab × Vtrab)/TV = 1050.3 Kg/m^3 [35].

The other important property of the bone is its mechanical characteristic. Finding a correct value for the elastic modulus of the homogeneous bone is very difficult as it depends not only on the elastic moduli of the cortical and trabecular bone but also on the geometry of the model. Thus, for the elastic modulus and the Poisson's coefficient, the values mentioned by other authors in a similar study [18] were used (E = 15 GPa, v = 0.3).

Once the values of the physical parameters of the model have been established, we proceeded to its implementation in the ANSYS v19.0 software [35]. The Static Structural analysis system from Workbench was used. After importing it from GrabCAD, the geometry

was discretized by ANSYS Meshing into 231,353 tetrahedral elements, 10^{-3} m in size. The resulted surface mesh of the model is illustrated in Figure 2.

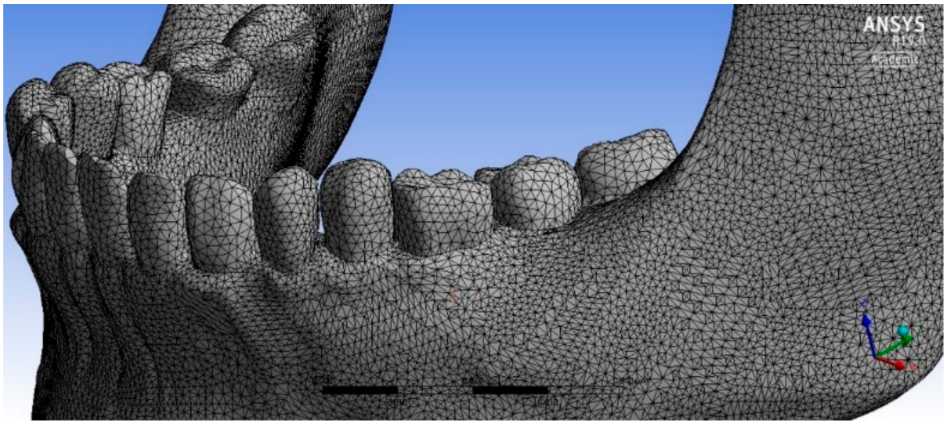

Figure 2. The mandible model's tetrahedral finite element network.

2.2. Mechanical Stress Simulation

With the geometry and the mechanical properties of our mandibular model already defined, two types of static loads were applied.

First, the forces generated by the three primary muscles involved in the mastication process, namely the temporal, masseter, and median pterygoid were applied to the mandible to simulate its normal loading conditions. The values and the orientations of these forces were taken from the study by Gregolin et al. [18]. The surfaces on which each of the six muscles acts have been established approximately, based on the information about their areas of insertion gathered from textbooks about the anatomy and physiology of the stomatognathic system. To complete the setup for the simulation of the mastication process, the conditions for a frontal bite have been imposed. Specifically, while the second premolar and the three molars on either side of the mandible were moving freely, the displacement of the four incisors of the two canines and first premolars was restricted by the presence of a stiff object. The greater the stiffness of the object, the greater the intensity of the bite. Figure 3 illustrates the boundary conditions applied for the simulation of a normal frontal bite.

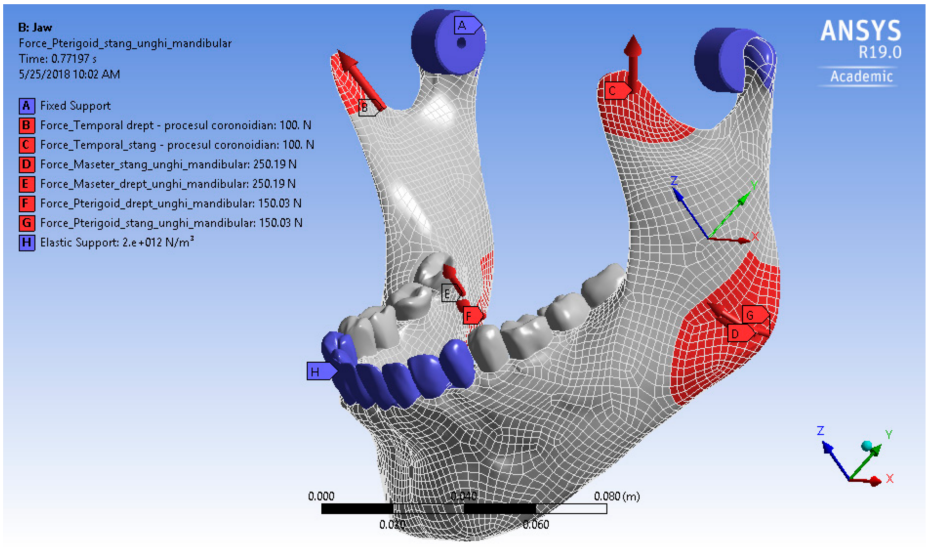

Figure 3. The boundary conditions for the frontal bite model. A: fixed support; B–G: forces from the masticatory muscles; H: elastic support.

With the second type of loading, we attempted to simulate the stresses developed in the mandible by impact forces. The most vulnerable places for jaw impact in traumatic conditions were considered as follows: the chin (in the case of a fall or a frontal hit) and the lateral area of the jaw (in the case of a fall or a side impact). In both cases, the mouth was closed, and the masticatory muscles relaxed. Thus, the only forces applied to the mandible were those due to impacts. The temporomandibular joints were fixed, and the forces were delivered either in the chin area or on the right side of the jaw.

The impact force (F) was applied perpendicular to an arbitrary surface of area Sb = 10^{-3} m^2 located in one of the two positions mentioned above. The amount of force corresponding to the fall of a five-kilogram body (the head), from a height of two meters is given by (F = 6666.7 N). We considered that, during the impact, the movement of the teeth in the mandible was restricted by the teeth in the upper jaw. For this, the boundary condition applied to the teeth was that of an elastic support with the foundation stiffness of 2 × 10^{12} N/m^3, the same as the stiffness of the teeth. Special attention was paid to the incomplete dentition. In those cases, because the "missing" teeth have not been removed from the model, their surfaces were set free to move. Figure 4 illustrates the boundary conditions applied for the simulation of a chin impact with missing teeth.

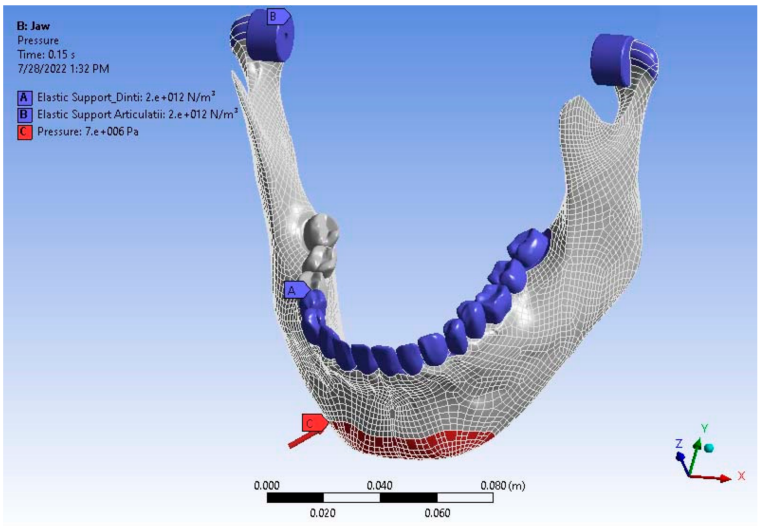

Figure 4. The boundary conditions for the frontal (chin) impact with three missing teeth (first, second and third molars). A: elastic support teeth; B: elastic support temporomandibular joints; C: pressure 7 × 10^6 Pa.

The convergence of the solution was determined by the mesh density. No adaptive mesh has been used due to the limitations in computational power.

Using this model, multiple scenarios have been investigated. Impact on the chin region, in an anteroposterior direction, and lateral impact on the mandible, from the basilar edge to the gonion were examined. The picture of possible clinical situations investigated in our study was extended by also considering several cases of incomplete dentition: (1) mandibular complete dentition; (2) jaw with missing mandibular molars; (3) jaw with missing third molar and first and second premolars; (4) jaw with missing canine, third molar, first and second premolars and (5) complete edentation.

Each of the eleven simulated clinical situations were analyzed and discussed from the point of view of the total deformation and the equivalent (von-Mises) stress induced on the surface of the mandible. Special attention was paid to the region of the condyle.

3. Results

3.1. Normal Bite

The first simulated scenario involved the six masticatory muscles acting and the eight front teeth (four incisors, two canines, and the two first premolars) pressing on a stiff body

(frontal bite). The remaining 6 teeth (two second premolars and four molars) were free to move (Figure 5a,b).

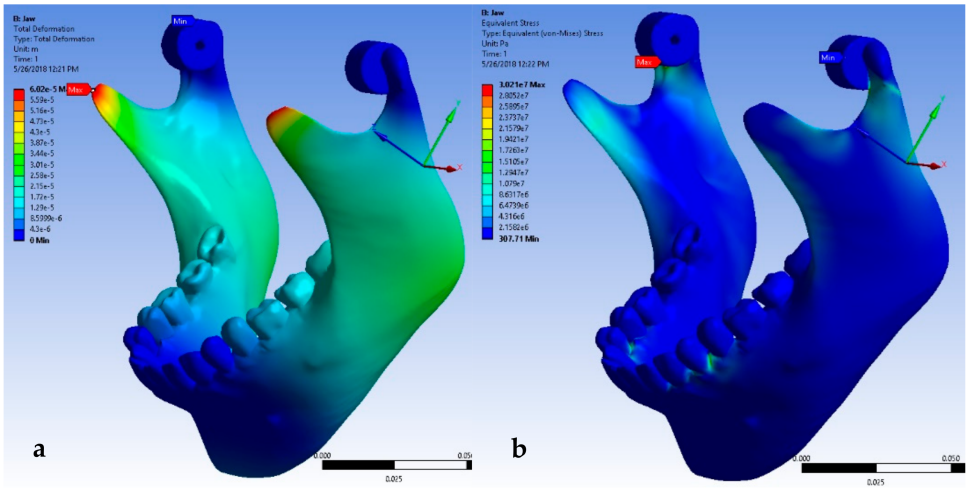

Figure 5. Mandible deformation (**a**) and Von Mises jaw stress (**b**) caused by a frontal bite from an item with rigidity of 2×10^{12} N/m^3: the coronoid process's extremity had the most deformations; the condylar process and the front portion of the mandible had the least amount of deformation. Additionally, there were high stress values in the region of the gap between the lower premolars. 30.21 MPa was the maximum stress value (von Mises stress).

3.2. Impact Response

3.2.1. Impact on the Chin Region

The jaw deformation and stress values in the impact on the chin and five alternative clinical scenarios compared to normal bite conditions were summarized in Table 1.

Table 1. Total deformation and equivalent stress on the surface of the condyle, in case of impact on the anterior face of the chin region.

Case	Scenario	Deformation [mm]	Stress [MPa]
Normal bite	Complete dentition	0.02	4.3
Impact on the anterior region, in the chin area	Complete dentition	0.01	9.6
	Missing first, second and third molars	0.02	25
	Missing third molar and first and second premolars	0.01	13.4
	Missing third molar, first and second premolars, and canine	0.01	13.65
	Complete edentation	1.6	1300 (>180)

The impact on the chin region increased the mechanical stress on the jaw but none of the stress levels found exceeded the fracture limit of 180 MPa except for complete edentation. The biggest deformations were noticed at the end of the coronoid process. The area between the two premolars had high-stress levels as well. The condylar process and the front of the mandible had the fewest deformations, and the highest stress was 30.21 MPa (below the flow limit of 180 MPa). A characteristic stood out in all the cases studied thus far: the concentration of strain around the base of the teeth that are present on the mandible jaw. If we considered the mechanics of the impact, we may expect that the fracture will involve the alveolar sockets of the teeth with no supporting basis for the teeth.

Impact on the Chin with Mandibular Complete Dentition

The outcome of Figure 6 was produced in impact on the chin with mandibular complete dentition, which was expressed as total deformation and equivalent stress (von Mises

stress). The largest deformation (about 0.16 mm) was detected in the chin protuberance, and the maximum tension (about 34 MPa) was observed in the area between premolars. In the area of the condylar process, a value of 33 MPa was found.

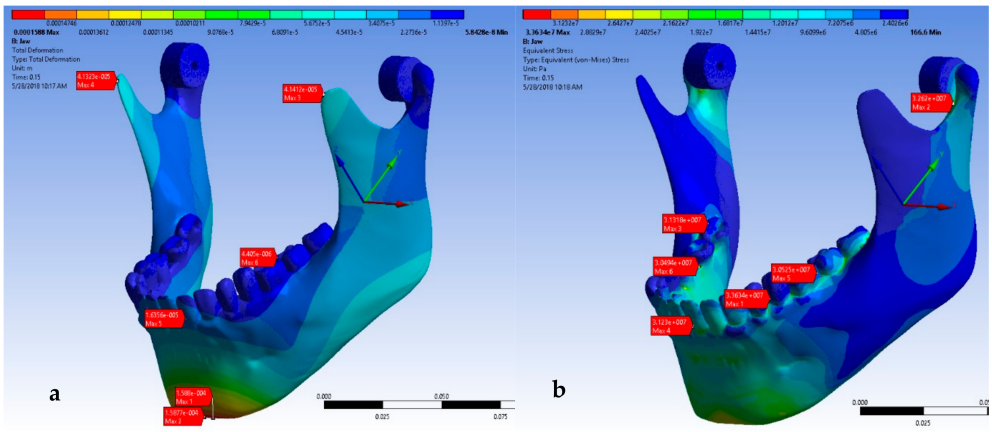

Figure 6. Total deformation (**a**) and equivalent stress distributions (the chin protuberance experienced the greatest deformation, nearly 0.16 mm) (**b**) on the mandible's surface in the event of a collision with the anterior face of the chin region, with complete dentition. The premolar region experienced the highest stress, (approximately 34 MPa), and the condylar process region experienced a close value, of 33 Mpa.

Impact in the Chin Region of the Jaw with Missing Mandibular Molars

The total strain and stress distributions in the chin region in the jaw with missing mandibular molars are shown in Figure 7. A large concentration of stress can be detected on the right side of the mandible (homolateral jaw), in the area between the missing molars and premolars, as seen in Figure 7b. The maximum values of the ensuing stress in this area were approximately 2.5 times higher than in the case of the same impact forces on the jaw with complete dentition (88 Mpa compared to 33 Mpa). None of the stress levels found exceeded the fracture limit of 180 Mpa. The maximal distortion, which also occurred in the chin protrusion area, was slightly increased compared to the complete dentition scenario (0.19 mm compared to 0.16 mm in the case of complete dentition). The stress value in the condyle area was also lower than the fracture limit (25 Mpa), and the deformation was quite minor (0.026 mm).

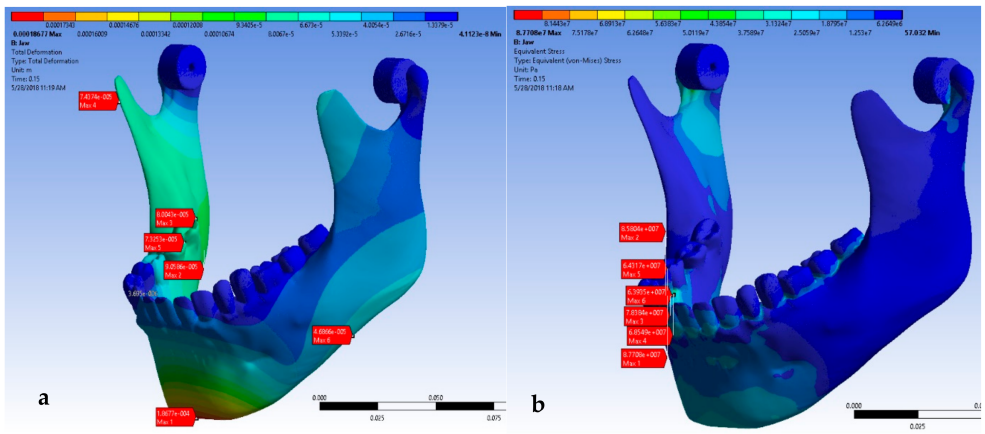

Figure 7. Distributions of total deformation (**a**) and equivalent stress (**b**) on the surface of the mandible in the event of an impact on the anterior face of the chin region in the absence of first, second, and third molars. The area of the mental protuberance showed the highest deformation, 0.19 mm. The condyle area had a stress value of 25 MPa and little deformation of 0.026 mm.

Impact in the Chin Region of the Jaw with Missing Third Molar, First and Second Premolars

The results were identical in terms of the position of the deformation and stresses in the absence of the lower premolars. High stresses are present in missing teeth (47 Mpa), but the values were lower than they were in the case of missing molars.

Impact in the Chin Region of the Jaw with Missing Canine, Third Molar, First and Second Premolars

The loss of the third molar, the first and second premolars, and the canine was the next examined clinical scenario. The changes were minor in the case of canine absence compared to previous cases. Maximum stresses were less than 47 Mpa. The stress in the condyle area was 13.65 Mpa, and the deformation was 0.0118 mm.

Impact in the Chin Region of Mandible with Complete Edentation

If all the teeth were missing and the mandible's body could move freely, the strains occurring in the condylar process were assessed. In the circumstances described above, the two images in Figure 8 show the distributions of the two sizes of interest, total deformation, and equivalent stress on the surface of the mandible. In case of no occlusal stops, the mandibular jaw, and condylar process take on all the stress. The vertical rim of the mandible encounters a lot of deformation, and the mechanical stresses were substantially higher than the bone fracture limit. The maximum stress values obtained from the calculations reach around 1.3 Gpa, which was approximately ten times greater than the fracture threshold and positioned at the base of the condyles. Violent chin movement of approximately 2.3 cm related to normal position can result in condylar fracture or dislocation (Figure 8).

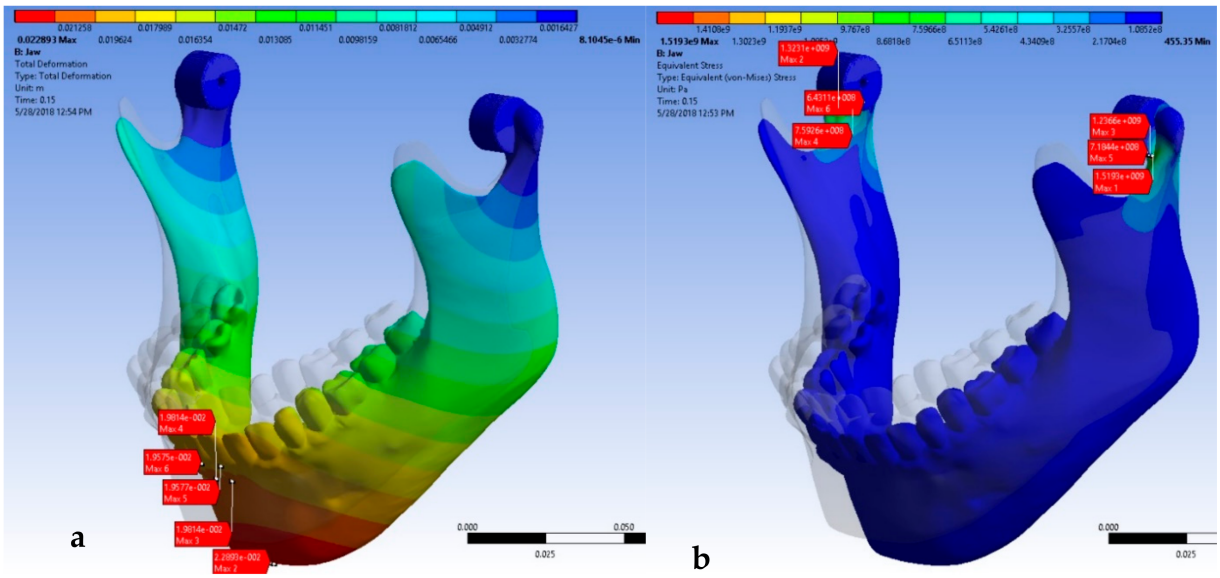

Figure 8. Deformation (**a**) and stress distribution (**b**) on the surface of the mandible in case of impact on the anterior face of the chin region (fractured teeth) in the mandibular complete edentation. The condylar process and the ramus of the mandible retained all the stress.

3.2.2. Impact on the Lateral Area of the Mandible

The jaw deformation and stress values in the impact on the lateral area of the mandible and five alternative clinical scenarios compared to normal bite conditions are summarized in Table 2. The impact at the level of gonion and ascending ramus increased the mechanical stress on the surface of the condyle but none of the stress levels found exceeded the fracture limit of 180 MPa in normal bite conditions. Total deformation and stress on the condyle surface were much closer to each other than the impact on the anterior face of the chin region, and all stress values exceed the limit value above which the mandible fracture can occur in

the condyle. The highest values are found for the case of complete edentation (860 MPa); and in the case of missing first, second, and third molars (662 MPa). It is worth noting that they are close to each other and are significantly larger than in previous occurrences. In the case of total edentation, the stress in the area of the condyle on the side where the external force operates was 860 MPa, while on the opposite side is roughly 300 MPa, i.e., almost three times lower, but both determined values surpassed the strength limit of 180 MPa.

Table 2. Total deformation and equivalent stress on the surface of the condyle, in case of impact on the lateral area, at the level of the gonion, and the ascending ramus.

Case	Scenario	Deformation [mm]	Stress [MPa]
Normal bite	Complete dentition	0.24	109.04
Impact on the lateral region, at the level of the gonion and the ascending ramus	Complete dentition	1.3	662
	Missing first, second and third molars	0.7	240
	Missing third molar and first and second premolars	0.7	241.5
	Missing third molar, first and second premolars, and canine	1.35	860
	Complete edentation	0.24	109.04

Lateral Impact on the Mandible in the Jaw with Complete Dentition

In this situation, the equivalent stress (von Mises stress) and total deformation were calculated, yielding the result shown in Figure 9. The stress in the condyle area was calculated to be 109.04 MPa, and the deformation in the same area was 0.24 mm, yet none of the stress levels found was more than 180 MPa the fracture limit.

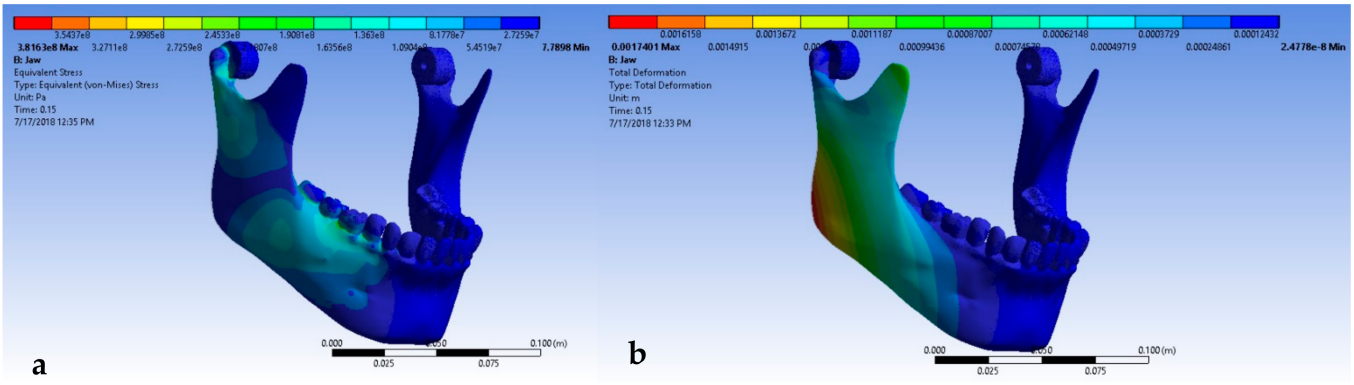

Figure 9. Equivalent (**a**) stress distributions (unit: Pa) and (**b**) total deformation (unit: Pa) on the mandible's surface in the event of a lateral impact with complete dentition: equivalent (von Mises stress) stress, time: 0.15 s.

Lateral Impact on Mandible with Missing First, Second and Third Lower Molar

The maximal stress in the condylar region was found to be 662 MPa. It was found that when an external force occurred on the jaw at the level of the gonion and ascending ramus, the resistance limit value (180 MPa) was exceeded, and the mandible yielded in the condyle area. Figure 10 depicts a detail of the stress in the condyle area (Figure 10a), as well as the distribution of stress on the mandible in the posterior view, to emphasize this point (Figure 10b).

Lateral Impact on Mandible with Missing Third Molar, First and Second Premolars

The stress in the condyle area was 240 MPa, which was 2.75 times lower than in the preceding situation (missing first, second, and third molars). However, this value was 1.33 times greater than the limit threshold, which could result in another mandible fracture. The highest deformation was next to the gonion and next to the condyle had a value of 0.7 mm.

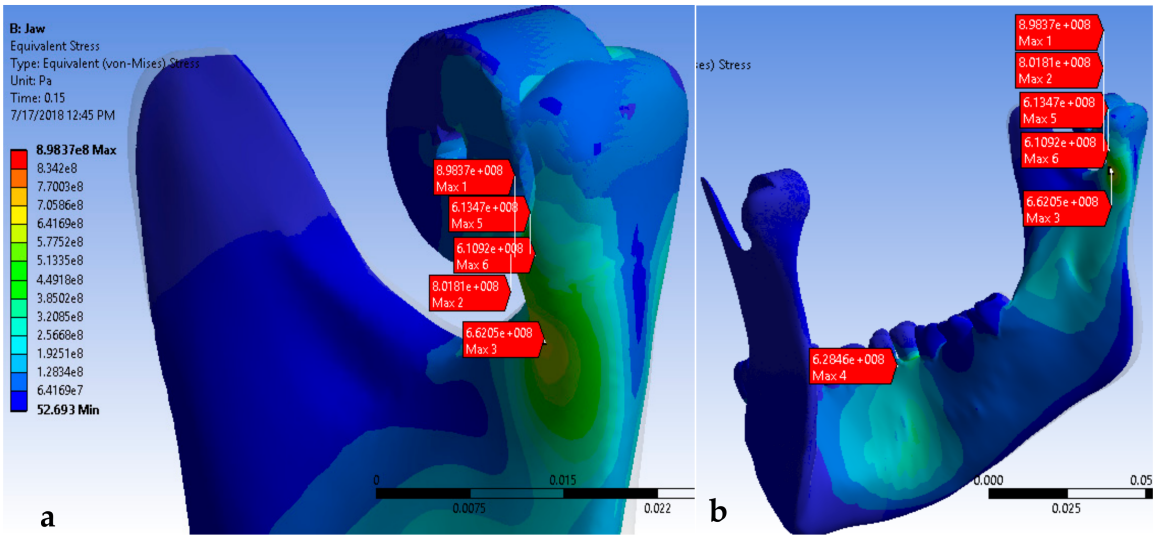

Figure 10. Stress distribution in the absence of first, second, and third molars: (**a**) condyle detail; (**b**) posterior view of the mandible: equivalent (von Mises stress) stress, unit: Pa, time: 0.15 s.

Lateral Impact on Mandible with Missing the Third Molar, First and Second Premolars, and Canine

The lack of the third molar, first and second premolars, and canine was the next examined clinical scenario. The following were the values of the sizes of interest in the condyle area: the stress was 241.5 MPa and the deformation was 0.7 mm. The two sums of interest were quite similar, if not identical, to those in the prior situation.

Lateral Impact on Mandible with Complete Edentation

The stress in the condyle area on the side where the external force operates was 860 MPa, whereas the stress in the condyle on the other side was roughly 300 MPa or about three times lower. Both results, however, exceeded the strength limit of 180 MPa (Figure 11). According to Figure 11b, the deformation in the condyle area was 1.35 mm in this situation.

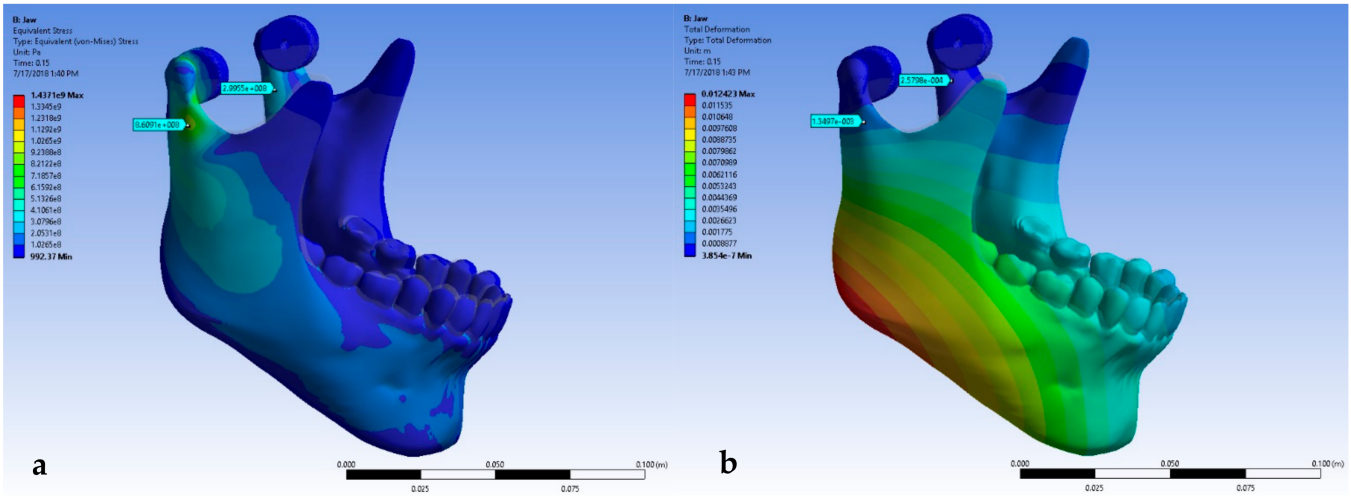

Figure 11. (**a**) Equivalent stress (unit: Pa) and (**b**) total deformation distributions (unit: m) on the mandible's surface in the event of a lateral face impact and complete edentation: equivalent (von Mises stress) stress, time: 0.15 s.

3.3. Impact Stress with Edentation on Both Hemiarches

We explored scenarios in which an external force acted on the chin or the side of the mandible, in the gonion area, but the edentation was symmetrical on both sides of the mandible. A comparison was made between the stress values obtained for these cases, both for an external force applied in the chin area and for one applied laterally; the corresponding stress values for edentation on a hemiarch, to emphasize the importance of considering the cases studied for impact stress, with edentation on both hemiarches. Table 3 summarizes the stress values for all the above scenarios. The stress values in equivalent conditions (edentation on a hemiarch versus symmetrical edentation) are extremely similar, both in the case of impact on the front face, in the chin region, and the case of impact on the side, at the gonion and ascending ramus. This could potentially be due to a measuring error while using the mouse to select the measurement location. The ability to take measurement samples from the same unitary defined region, per condyle, as an average of the values of the individual points would be useful.

Table 3. Comparative stress values [MPa].

Scenario	Impact on the Anterior Side, in the Chin Region		Impact on the Lateral Side, on the Angle of the Mandible	
	Edentation on One Hemiarch	Symmetrical Edentation	Edentation on One Hemiarch	Symmetrical Edentation
Missing first, second and third molars	25	25.29	662	659
Missing third molar, first and second premolars, and canine	13.65	13.51	241.5	241.5

3.3.1. Impact on the Chin in the Mandible with Bilateral Edentation on the Molar Region

In this situation, the force that acts on the chin region when the first, second, and third molars are absent is shown in Figure 12. The following stress values were deduced: the outside of the condyle had a pressure of 25.29 MPa, whereas the inside had a pressure of 19.12 MPa.

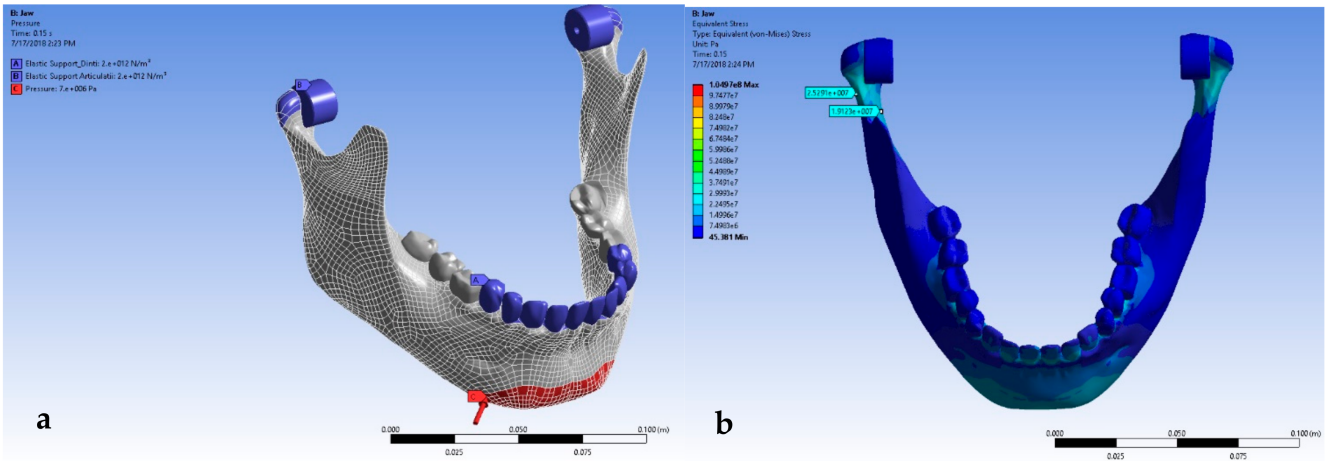

Figure 12. (**a**). If both hemiarches' first, second, and third molars are absent, the force acts on the anterior face of the chin region (A-elastic support teeth 2×10^{12} N/m^3; B-elastic support joint 2×10^{12} N/m^3; C-pressure 7×10^7 Pa). (**b**) The equivalent stress on the surface of the mandible in case of impact on the anterior chin region, with the lack of first, second, and third molars on both hemiarches: equivalent (von Mises stress) stress, unit: Pa, time: 0.15 s.

3.3.2. Impact on the Chin in the Mandible with Bilateral Edentation on the Molar, Premolar Region, and Canine

The value of stress in the condyle area is 13.51 MPa, which is extremely similar to the value obtained in the same force action circumstance, with the exception that one hemiarches' tooth was absent.

3.3.3. Lateral Impact on the Mandible with First, Second, and Third Molars Missing on Both Hemiarches

The three stress values on the labels are worth noting: 417.34 MPa on the outer surface of the condyle on the same side as the region of force action, 659 MPa on the inner surface of the same condyle, and 335.6 MPa on the opposite side of the force area. All stress values were higher than the resistance limit value, with the maximum being on the inner area of the condyle, which is on the same side as the area of external force actuation.

3.4. Lateral Impact on the Mandible with the Third Molar, First and Second Premolars, and Canine Absence on Both Hemiarches

The stress at the condyle measured 241.5 MPa.

4. Discussion

Finite element analysis is used in dentistry in various fields: to assess the biomechanical performance of crown veneers built of zirconia [36], to assess the impact of implant abutment contact surfaces and abutment screw torque on the development of stress [37] or to assess how cement thickness affects the adhesively cemented composite inlays' polymerization shrinkage stress [38].

Following the steps outlined in this paper, the following statements can be derived. The impact on the anterior area of the mandible causes total deformation and stress on the condyle surface which are not dangerous, as they were far below the permissible limit values, with the concentration of stress at the base of the teeth. In the case of total edentulousness, the value of the stress in the condyle area exceeded more than ten times the permissible value of the resistance limit (180 MPa), resulting in mandibular fracture.

The impact on the side, at the level of the gonion and the ascending ramus, loads a higher stress value that exceeds the limit value above which the mandible in the condyle area may fracture. The highest values were found for complete edentation (860 MPa) and in the absence of first, second, and third molars (662 MPa). They were close together and significantly larger than in previous occurrences.

In the case of total edentation, the stress around the condyle on the side where the external force operates was 860 MPa, while on the opposite side was roughly 300 MPa, i.e., almost three times lower, but both determined values surpassed the strength limit of 180 MPa.

It was shown that the stress levels in analogous conditions, i.e., for the same type of impact but with edentation on one hemiarch and subsequently with symmetrical edentation on both hemiarches, were quite nearby. The results are 25.29 MPa (symmetrical edentation) and 25 MPa (lack of first, second and third molars) in the case of an impact on the chin area and the lack of first, second, and third molars, respectively (edentation on a hemiarch). This could potentially be due to a measuring error while using the mouse to select the measurement location.

Two three-dimensional models of the mandible were created using the software ANSYS v19.0 and the finite element (FE) method to complete the task. The initial model, which was designed to replicate the mastication process, included forces exerted by the primary muscles involved: the temporal, masseter, and medial pterygoid. The forces imposed by the masticatory muscles were eliminated in the second model and were replaced by stronger stresses imposed by external, frontal, and lateral impacts.

Drăgulescu D. employs the FE method in a study but also uses MathCAD to generate a simpler model by solving a system of differential equations (classical mechanical method). The two models also differ in that one has a simplifying hypothesis, which is represented

by the cancellation of the temporalis muscle's action, whilst the other, as in our situation, is much closer to reality [39].

Several groups of researchers have used this method, and, the FE method, is being employed as a mathematical foundation [14,40–42]. The software employed and the accuracy of the results, given the model's resolution, are what set this research apart (the number of finite elements in which the outer surface of the mandible is divided).

Except for Tanaka et al. who leveraged the camera's capabilities, all of the authors used three-dimensional (3D) scanners to acquire basic data on the mandible [42]. For the 3D model of the mandible to be realized, these data were transformed to generate a jaw contour, either using a specialized program, Mimics, used by Szucs et al. or by a program built-in Fortran Hart et al. either by using ANSYS as in this paper, or by utilizing Simail (France), or by using the Patran (USA) program [14,35,40,41].

It was shown by Choi et al. that the outer surface of the mandible must be divided into at least 30,000 finite elements to obtain an analysis with a high degree of precision [23]. While the number of elementary tetrahedra described by Gallas Torreira et al. was 30,119 and only a few thousand by Tanaka et al. the models created for this research comprised 231,353 such elements, resulting in significant discrepancies in values for the sizes desired [14,42].

We have adopted the same physical sizes for the mandibular bone's characteristic sizes, namely the density, which was measured in kg/m^3, the modulus of elasticity, E, which was measured in MPa or GPa, and the Poisson's dimensionless ratio. The numbers described by Gallas Torreira et al. which were also employed in the current paper, to create the model for simulating the mastication process, were used as values [14]. The partial volumes of cortical and trabecular tissue, respectively, had to be determined in this scenario. The values used for a homogenous bone structure, which were employed in the second model, in the biomechanical investigation of the mandible on impact, have been also reported by Gregolin et al. and Gallas Torreira et al. [14,18].

Mandibular head fractures are important to consider, as different injury mechanisms demand various therapeutic modalities, a treatment method being the surgical approach, in which compression osteosynthesis-specific screws have been created. The therapeutical success depends on the location of the fracture and on knowing where to place the fixation due to the small size of the fractured bones [43]. Kozakiewicz et al. stated that despite the publication of 30 plate designs, no information on plates for low-neck mandibular condylar osteosynthesis can be found, therefore the authors compared different types of specialized plates that might be used in low-neck condylar fracture osteosynthesis [43,44]. In their study of low-neck mandibular condylar osteosynthesis plates, the authors found that one should either take into account the mechanical benefits when selecting a plate for open rigid internal fixation in low-neck condylar fractures, or one should only be aware of the notable variations in mobility within the fracture line after fixation with different specialized plates [44]. Moreover, condylar hypertrophy should be considered before treatment planning [45].

In other situations, an acrylic splint was used by the authors to functionally realign the mandible in a case of unilateral mandibular subcondylar fracture with dislocation [46]. Moreover, it is possible to use teledentistry to supplement conventional treatment for various oral diseases and it is crucial to consider the cause-and-effect implications and treatment planning techniques [47,48].

Some authors have chosen either a complete dentition or an asymmetrical structure on the two hemiarches, i.e., missing molars on the left, molars, premolars, and canine on the right, or simply the third molar, with various procedures around it depending on the aim [40–42].

It is also possible that the way impact attributes are defined differs. As a result, Syed et al. used a one-second duration, whereas, in the current study, it was 15 milliseconds. The location and surface on which the hit is regarded, as well as the pressure with which was applied, are all determined by the author's goal [22].

In terms of the goal, some authors want to create a three-dimensional model of the dental mandible to study and analyze the mechanical stresses that occur during normal mastication while others want to determine areas of maximum stress, for various external actions and dentition structures, to prevent fractures without being specifically dedicated to a goal [14,39,40,42].

The goal of Szucs et al., was to determine the effects of certain procedures in specific parts of the mandible (M3 molar) [41].

The following points should be noted concerning the outcomes: a reasonable approximation of results between this study and those of the authors [41]. In some cases, for example, in the situations described by Szucs et al., the stress was in the range of 9–27 MPa, at various points of the mandible, whereas in this study, the stress of 25 MPa was determined in the condyle area [41]. The greatest stress that occurred for an impact in the lateral area (of the same amount) was described by Szucs et al., on the condyle, as it is in our case [41]. The stress values obtained for the prior example, described by Gallas Torreira et al. were 50–808 MPa and up to 860 MPa in the current study [14].

5. Limitations and Strengths

Nevertheless, the other quality criteria were fulfilled. A large number of mechanical stress simulations in the normal bite as well as the impact on the chin region, on the forehead, and on the angle and vertical rim of the mandible, with missing mandibular molars, missing the third molar, first and second premolars, missing canine, third molar, first and second premolars and complete edentation brings new data on mechanical simulation of the various clinical situations under impact conditions.

The main goal of this paper was to examine the biomechanical behavior of the mandible, particularly in the condyle area, in conditions that are considered representative of human dentition, including complete dentition but also certain cases of edentulousness, both in the case of normal bite and in the case where the mandible is subjected to certain types of simulated loads, such as impact in the chin area and ascendent ramus. The following is recommended as a continuation of this study and to complete it with additional data while also enhancing the reliability of the data: To increase the number of cases of external force action; to make comparison measurements at the same points, defined as a unit by the same coordinates; to take measurement samples from the same area, defined in units, per condyle, as an average of the values of the individual points.

6. Conclusions

In conclusion, the presence of a normal bite and the direction of the impact forces influence the deformation of the mandibular bone and its risk of fracture.

In the case of anterior impact, the frontal area of the mandible and the condylar process had the smallest deformation with a low risk of fracture. In the case of total edentulousness mandibular jaw, the value of the stress in the condyle area and the permissible value of the resistance limit could lead to mandible fracture.

In the case of lateral impact, all stress values were greater than the threshold value at which the mandible's condyle region is susceptible to fracture. The stress levels for the lateral impact within unilateral or bilateral mandibular edentation were quite nearby. More research on this subject is required to improve its clinical significance. Future studies with multiple scenarios of external force levels related to various bone densities and the absence of dental units could be also considered.

Author Contributions: Conceptualization, M.H. and D.G.P.; methodology, S.G.P.; software, S.G.P. and D.R.; validation, M.H., H.H. and S.G.P.; formal analysis, M.H. and D.G.P.; investigation, S.G.P.; resources, S.G.P.; data curation, D.G.P.; writing—original draft preparation, O.A.; writing—review and editing, O.A. and M.H.; visualization, M.H. and H.H.; supervision, M.H.; project administration, M.H. All authors have read and agreed to the published version of the manuscript.

Funding: This research received no external funding.

Institutional Review Board Statement: Not applicable.

Informed Consent Statement: Not applicable.

Data Availability Statement: The data presented in this study are available from the last author upon reasonable request.

Conflicts of Interest: The authors declare no conflict of interest.

List of Abbreviations

Temporomandibular joint (TMJ); Finite element (FE); Bone body (TV); Bone matrix (MV); Volume of the cancellous bone spaces (VS); Volume fraction (VF); Porosity volume (pV); Surface area (SA); Volume fraction (VF); Bone density (q); Density of the tissue of the bone matrix (qm); Density of the spaces of the bone matrix (qs); Average thickness of the cortical tissue (Hcort); Cortical bone volume (Vcort); Volume of the trabecular tissue (Vtrab); Density of the cortical tissues (qcort); Density of the trabecular tissues (qtrab); Average density (qave); Poisson's coefficient (v); Elastic modulus (E); Impact force (F); Giga Pascal (GPa); Computer Aided Design (CAD); Premolars (PMs); Molar (Ms); Canine (C).

References

1. Farzan, R.; Farzan, A.; Farzan, A.; Karimpour, M.; Tolouie, M. A 6-Year Epidemiological Study of Mandibular Fractures in Traumatic Patients in North of Iran: Review of 463 Patients. *World J. Plast. Surg.* **2021**, *10*, 71–77. [CrossRef] [PubMed]
2. Hassanein, A.G. Trends and Outcomes of Management of Mandibular Fractures. *J. Craniofacial Surg.* **2019**, *30*, 1245–1251. [CrossRef]
3. Dreizin, D.; Nam, A.J.; Tirada, N.; Levin, M.D.; Stein, D.M.; Bodanapally, U.K.; Mirvis, S.E.; Munera, F. Multidetector CT of Mandibular Fractures, Reductions, and Complications: A Clinically Relevant Primer for the Radiologist. *Radiographics* **2016**, *36*, 1539–1564. [CrossRef]
4. Algan, S.; Kara, M.; Cakmak, M.A.; Tan, O.; Cinal, H.; Barin, E.Z.; Inaloz, A. Experiences with a Modified Preauricular Mini Incision with Subdermally Dissection in Condylar and Subcondylar Fractures of the Mandible. *J. Cranio-Maxillofac. Surg.* **2018**, *46*, 588–593. [CrossRef]
5. Bertin, E.; Louvrier, A.; Meyer, C.; Weber, E.; Barrabé, A. Pons An Epidemiologic Retrospective Study of Maxillofacial Traumatology in the Elderly. *J. Stomatol. Oral Maxillofac. Surg.* 2022, *in press*. [CrossRef]
6. Abukhder, M.; Mobarak, D. A Retrospective Cohort Study on the Aetiology and Characteristics of Maxillofacial Fractures Presenting to a Tertiary Centre in the UK. *Ann. Med. Surg.* **2022**, *77*, 103622. [CrossRef]
7. Pickrell, B.; Serebrakian, A.; Maricevich, R. Mandible Fractures. *Semin. Plast. Surg.* **2017**, *31*, 100–107. [CrossRef] [PubMed]
8. Sattar, N.; Gillani, S.R.R.; Erkin, M.; Khan, M.; Abbas, M.; Khurshid khattak, N. Role of Environmental and Occupational Factors in Fall-related Maxillofacial Fractures. *Clin. Exp. Dent. Res.* **2022**, *8*, 737–774. [CrossRef] [PubMed]
9. Sorenson, T.J.; Borad, V.; Schubert, W. A Nationwide Study of Skiing and Snowboarding-Related Facial Trauma. *Craniomaxillofac. Trauma Reconstr.* **2022**, *15*, 28–33. [CrossRef]
10. Diab, J.; Moore, M.H. Patterns and Characteristics of Maxillofacial Fractures in Women. *Oral Maxillofac. Surg.* **2022**, 1–10. [CrossRef]
11. Li, J.; Jiao, J.; Luo, T.; Wu, W. Biomechanical Evaluation of Various Internal Fixation Patterns for Unilateral Mandibular Condylar Base Fractures: A Three-Dimensional Finite Element Analysis. *J. Mech. Behav. Biomed. Mater.* **2022**, *133*, 105354. [CrossRef]
12. Avci, T.; Omezli, M.M.; Torul, D. Investigation of the Biomechanical Stability of Cfr-PEEK in the Treatment of Mandibular Angulus Fractures by Finite Element Analysis. *J. Stomatol. Oral Maxillofac. Surg.* 2022, *in press*. [CrossRef]
13. Graillon, N.; Guyot, L.; Thollon, L.; Godio-Raboutet, Y.; Roux, M.-K.L.; Foletti, J.-M. Do Mandibular Titanium Miniplates Affect the Biomechanical Behaviour of the Mandible? A Preliminary Experimental Study. *J. Stomatol. Oral Maxillofac. Surg.* 2022, *in press*. [CrossRef]
14. Torreira, M.G.; Fernández, J.R. A Three-Dimensional Computer Model of the Human Mandible in Two Simulated Standard Trauma Situations. *J. Cranio-Maxillofac. Surg.* **2004**, *32*, 303–307. [CrossRef]
15. Gomez, M.A.; Nahum, A.M. Biomechanics of Bone. In *Accidental Injury*; Nahum, A.M., Melvin, J.W., Eds.; Springer: New York, NY, USA, 2002; pp. 206–227, ISBN 978-1-4419-3168-9.
16. Carter, D.R.; Spengler, D.M. Mechanical Properties and Composition of Cortical Bone. *Clin. Orthop.* **1978**, *135*, 192–217. [CrossRef]
17. Burstein, A.H.; Reilly, D.T.; Martens, M. Aging of Bone Tissue: Mechanical Properties. *J. Bone Jt. Surg. Am.* **1976**, *58*, 82–86. [CrossRef] [PubMed]
18. Gregolin, R.F.; de Carvalho Zavaglia, C.A.; Tokimatsu, R.C.; Pereira, J.A. Biomechanical Stress and Strain Analysis of Mandibular Human Region from Computed Tomography to Custom Implant Development. *Adv. Mater. Sci. Eng.* **2017**, *2017*, 7525897. [CrossRef]
19. Turner, C.H.; Burr, D.B. Basic Biomechanical Measurements of Bone: A Tutorial. *Bone* **1993**, *14*, 595–608. [CrossRef]
20. Kimsal, J.; Baack, B.; Candelaria, L.; Khraishi, T.; Lovald, S. Biomechanical Analysis of Mandibular Angle Fractures. *J. Oral Maxillofac. Surg.* **2011**, *69*, 3010–3014. [CrossRef]

21. Jung, B.T.; Kim, W.H.; Park, B.; Lee, J.-H.; Kim, B.; Lee, J.-H. Biomechanical Evaluation of Unilateral Subcondylar Fracture of the Mandible on the Varying Materials: A Finite Element Analysis. *PLoS ONE* **2020**, *15*, e0240352. [CrossRef]
22. Syed, I.; Joshi, A.; Desai, A.K.; Anehosur, V. Occlusal Analysis Using T-Scan in Patients with Condylar Fractures When Managed by Closed Method. *J. Craniofac. Surg.* **2020**, *31*, e451–e459. [CrossRef] [PubMed]
23. Choi, T.J.; Chung, Y.H.; Cho, J.Y.; Burm, J.S. The Use of Microplates for Internal Fixation of Comminuted Mandibular Fractures. *Ann. Plast. Surg.* **2019**, *82*, 55–61. [CrossRef] [PubMed]
24. Datarkar, A.; Tayal, S.; Thote, A.; Galie, M. An In-Vitro Evaluation of a Novel Design of Miniplate for Fixation of Fracture Segments in the Transition Zone of Parasymphysis-Body Region of Mandible Using Finite Element Analysis. *J. Cranio-Maxillo-fac. Surg.* **2019**, *47*, 99–105. [CrossRef] [PubMed]
25. Singleton, C.; Manchella, S.; Nastri, A.; Bordbar, P. Mandibular Fractures—What a Difference 30 Years Has Made. *Br. J. Oral Maxillofac. Surg.* 2022, *in press*. [CrossRef] [PubMed]
26. Kovacs, A.C.; Kaing, T.-L. Point-of-Care Computer-Assisted Design and Manufacturing Technology and Its Utility in Post-Traumatic Mandibular Reconstruction: An Australian Public Hospital Experience. *SAGE Open Med. Case Rep.* **2022**, *10*, 2050313X221103733. [CrossRef]
27. Huang, C.-M.; Chan, M.-Y.; Hsu, J.-T.; Su, K.-C. Biomechanical Analysis of Subcondylar Fracture Fixation Using Miniplates at Different Positions and of Different Lengths. *BMC Oral Health* **2021**, *21*, 543. [CrossRef]
28. Costa, F.W.G.; Bezerra, M.F.; Ribeiro, T.R.; Pouchain, E.C.; Sabóia, V.D.P.A.; Soares, E.C.S. Biomechanical Analysis of Titanium Plate Systems in Mandibular Condyle Fractures: A Systematized Literature Review. *Acta Cir. Bras.* **2012**, *27*, 424–429. [CrossRef]
29. Mańkowski, J.; Piękoś, J.; Dominiak, K.; Klukowski, P.; Fotek, M.; Zawisza, M.; Żach, P. A Mandible with the Temporomandibular Joint-A New FEM Model Dedicated to Strength and Fatigue Calculations of Bonding Elements Used in Fracture and Defect Surgery. *Materials* **2021**, *14*, 5031. [CrossRef] [PubMed]
30. WdoŁowski, P.; KrzesiŃski, G.; Gutowski, P. Finite Element Analysis of Mini-Plate Stabilization of Human Mandible Angle Fracture—A Comparative Study. *Acta Bioeng. Biomech.* **2020**, *22*, 105–116. [CrossRef]
31. Joshi, U.; Kurakar, M. Assessment of Lingual Stability in Mandible Fracture: Monocortical Versus Bicortical Fixation Using FEM Analysis. *J. Maxillofac. Oral Surg.* **2018**, *17*, 514–519. [CrossRef]
32. 3-Parts Anatomical Skull Model | 3D CAD Model Library | GrabCAD. Available online: https://grabcad.com/library/3-parts-anatomical-skull-model (accessed on 18 June 2022).
33. GrabCAD Making Additive Manufacturing at Scale Possible. Available online: https://grabcad.com/ (accessed on 18 June 2022).
34. Hart, N.H.; Nimphius, S.; Rantalainen, T.; Ireland, A.; Siafarikas, A.; Newton, R.U. Mechanical Basis of Bone Strength: Influence of Bone Material, Bone Structure and Muscle Action. *J. Musculoskelet. Neuronal Interact.* **2017**, *17*, 114–139.
35. ANSYS Products V19.0 Free Download {Full Version} for PC Windows. Available online: https://www.getintopces.com/ansys-products-v19-0-free-download/ (accessed on 18 June 2022).
36. Madruga, C.F.L.; Ramos, G.F.; Borges, A.L.S.; Saavedra, G.D.S.F.A.; Souza, R.O.; Marinho, R.M.D.M.; Penteado, M.M. Stress Distribution in Modified Veneer Crowns: 3D Finite Element Analysis. *Oral* **2021**, *1*, 272–280. [CrossRef]
37. Tribst, J.P.M.; Dal Piva, A.M.D.O.; da Silva-Concílio, L.R.; Ausiello, P.; Kalman, L. Influence of Implant-Abutment Contact Surfaces and Prosthetic Screw Tightening on the Stress Concentration, Fatigue Life and Microgap Formation: A Finite Element Analysis. *Oral* **2021**, *1*, 88–101. [CrossRef]
38. Campaner, L.M.; Alves Pinto, A.B.; Demachkia, A.M.; Paes-Junior, T.J.D.A.; Pagani, C.; Borges, A.L.S. Influence of Cement Thickness on the Polymerization Shrinkage Stress of Adhesively Cemented Composite Inlays: Photoelastic and Finite Element Analysis. *Oral* **2021**, *1*, 168–180. [CrossRef]
39. Dragulescu, D. Studierea Dinamicii Mandibulei si Modelarea de Implante Pentru Corectarea Prin Interventii Chirurgicale a Ruperilor Sale Accidentale. Available online: https://www.yumpu.com/en/document/view/53136953/studierea-dinamicii-mandibulei-si-modelarea-de-implante-pentru- (accessed on 19 June 2022).
40. Hart, R.T.; Hennebel, V.V.; Thongpreda, N.; Van Buskirk, W.C.; Anderson, R.C. Modeling the Biomechanics of the Mandible: A Three-Dimensional Finite Element Study. *J. Biomech.* **1992**, *25*, 261–286. [CrossRef]
41. Szucs, A.; Bujtar, P.; Sándor, G.; Barabás, J. Finite Element Analysis of the Human Mandible to Assess the Effect of Removing an Impacted Third Molar. *J. Can. Dent. Assoc.* **2010**, *76*, a72.
42. Tanaka, E.; Tanne, K.; Sakuda, M. A Three-Dimensional Finite Element Model of the Mandible Including the TMJ and Its Application to Stress Analysis in the TMJ during Clenching. *Med. Eng. Phys.* **1994**, *16*, 316–322. [CrossRef]
43. Kozakiewicz, M.; Gabryelczak, I. The Osteosynthesis of the Mandibular Head, Does the Way the Screws Are Positioned Matter? *J. Clin. Med.* **2022**, *11*, 2031. [CrossRef]
44. Kozakiewicz, M.; Zieliński, R.; Konieczny, B.; Krasowski, M.; Okulski, J. Open Rigid Internal Fixation of Low-Neck Condylar Fractures of the Mandible: Mechanical Comparison of 16 Plate Designs. *Materials* **2020**, *13*, 1953. [CrossRef]
45. d'Apuzzo, F.; Minervini, G.; Grassia, V.; Rotolo, R.P.; Perillo, L.; Nucci, L. Mandibular Coronoid Process Hypertrophy: Diagnosis and 20-Year Follow-Up with CBCT, MRI and EMG Evaluations. *Appl. Sci.* **2021**, *11*, 4504. [CrossRef]
46. Minervini, G.; Lucchese, A.; Perillo, L.; Serpico, R.; Minervini, G. Unilateral Superior Condylar Neck Fracture with Dislocation in a Child Treated with an Acrylic Splint in the Upper Arch for Functional Repositioning of the Mandible. *Cranio J. Craniomandib. Pract.* **2017**, *35*, 337–341. [CrossRef] [PubMed]

47. Minervini, G.; Russo, D.; Herford, A.S.; Gorassini, F.; Meto, A.; D'Amico, C.; Cervino, G.; Cicciù, M.; Fiorillo, L. Teledentistry in the Management of Patients with Dental and Temporomandibular Disorders. *BioMed Res. Int.* **2022**, *2022*, 7091153. [CrossRef] [PubMed]
48. Minervini, G.; Fiorillo, L.; Russo, D.; Lanza, A.; D'Amico, C.; Cervino, G.; Meto, A.; Di Francesco, F. Prosthodontic Treatment in Patients with Temporomandibular Disorders and Orofacial Pain and/or Bruxism: A Review of the Literature. *Prosthesis* **2022**, *4*, 253–262. [CrossRef]